

# Experimental and numerical studies on vertical properties of a new multi-dimensional earthquake isolation and mitigation device

Zhaodong Xu<sup>a,\*</sup>, Liheng Lu<sup>a</sup>, Benqiang Shi<sup>b</sup> and Fuhgwo Yuan<sup>c</sup>

<sup>a</sup>*Key Laboratory of Concrete and Prestressed Concrete Structures of the Ministry of Education, Southeast University, Nanjing, Jiangsu, China*

<sup>b</sup>*Guangdong Country Garden Holdings Limited Company, Foshan, Guangdong, China*

<sup>c</sup>*Department of Mechanical Engineering, North Carolina State University, Raleigh, NC, USA*

Received 25 April 2012

Revised 22 July 2012

Accepted 2 November 2012

**Abstract.** When designing critical structures such as long-span structures and high-rise buildings, earthquake excitation in the vertical direction, in addition to the horizontal direction, should also be taken into consideration. Study on new devices that can mitigate and isolate multi-dimensional (including both horizontal and vertical) earthquake actions has a remarkable significance. A new kind of multi-dimensional earthquake isolation and mitigation device was recently developed, and experimental study on vertical performances of the device under different excitation frequencies and amplitudes has been carried out in this paper. The characteristics of the vertical properties including the initial stiffness, the energy dissipation stiffness, the energy dissipation per cycle and the vertical damping ratio changing with excitation frequency and amplitude were studied, and the formulas describing the characteristics were proposed. It can be concluded that the initial stiffness and the energy dissipation stiffness increase slightly with increasing frequency, while the energy dissipation per cycle and the damping ratio decrease slightly with increasing frequency, the initial stiffness, the energy dissipation stiffness and the damping ratio will decrease slightly with increasing excitation amplitudes, and the proposed formulas can describe the vertical properties of the multi-dimensional earthquake isolation and mitigation device changing with excitation frequency and amplitude.

**Keywords:** Multi-dimensional, earthquake isolation and mitigation device, energy dissipation, viscoelastic, vertical properties, dynamic responses

## 1. Introduction

Earthquake can be considered as a complex multi-dimensional excitation covering horizontal, vertical and torsional components. Counter-measures of earthquake in both horizontal and vertical directions of important structures, such as long-span reticulated structures, bridges, high-rise buildings, should be considered [3]. The modern counter-measure of earthquake induced motion is to adopt control devices to mitigate earthquake responses. That is, some control devices are added in structures to isolate or dissipate earthquake energy for reducing earthquake responses of structures. A majority of the devices are studied to only reduce the horizontal earthquake responses

---

\*Corresponding author: Zhaodong Xu, Civil Engineering School, Southeast University, Si-Pai Lou 2#, Nanjing 210096, Jiangsu, China.  
E-mail: xuzhdgyq@seu.edu.cn.

of structures, while fewer devices are proposed to reduce the horizontal and vertical earthquake responses of structures simultaneously. To date, only a handful of multi-dimensional earthquake isolation or earthquake mitigation devices have been designed to mitigate dynamic responses of nuclear buildings, military buildings and precision instruments. A three-dimensional earthquake isolation device was proposed and tested under the horizontal and vertical loads, which consists of rubber bearing for horizontal earthquake isolation and sealed air cushion for vertical earthquake isolation [7]. A prototype multi-dimensional earthquake isolation device was recently developed for nuclear power station in Japan [5]. Multi-dimensional earthquake isolation device made up of hydraulic bearing and sway suppression air vats with rubber bearings beneath them was proposed based on the motive of providing both sufficient bearing capacity and effective suppression for swaying of structures for vertical earthquake isolation, static and dynamic tests for the scaled device were carried out [1]. Multi-dimensional earthquake isolation devices, which consist of rubber bearing or main bearing for horizontal earthquake isolation and damper springs for vertical earthquake isolation, had been recently studied [4,6,8].

This paper proposed a new kind of multi-dimensional earthquake isolation and mitigation device. This device has been awarded as a National Invention Patent in China with granted number: ZL03113392.4. The device consists of viscoelastic dampers and viscoelastic bearing, which can isolate and dissipate both horizontal and vertical vibration energy of structures. The properties of the device are acquired through horizontal and vertical property tests on the device. Horizontal tests and property analysis have been described in Reference [9]. Vertical tests and property analysis on this device under different excitation frequencies and amplitudes are carried out in detail in this paper. It can be concluded from the experimental and numerical results that the multi-dimensional earthquake isolation and mitigation device has a fine energy dissipation capability, and excitation frequency and amplitudes have significant effects on energy dissipation properties of the device.

## 2. Experimental set-up and procedure

### 2.1. Construction and working principles

Multi-dimensional earthquake isolation and mitigation device consists of viscoelastic isolation bearing, viscoelastic dampers and vertical springs, as shown in Fig. 1. For vertical vibration, viscoelastic bearing, viscoelastic dampers and springs constitute a vertical isolation system, where the stiffness is lower in comparison with other locations of structures. Mathematically the system resembles the Maxwell model. The device can isolate vertical vibration, at the same time, viscoelastic dampers and bearing can dissipate vibration energy when the device produces the relative displacement. Under minor earthquake, viscoelastic bearing dissipates a little vibration energy due to the slight loose-tight pressure movement of viscoelastic bearing. While under the strong earthquake, some columns and multi-dimensional earthquake isolation and mitigation devices may be tensioned. The springs in the device are pre-pressurized. If the tension force is smaller than the pressure of springs, the core bearing will contact with the upper steel plate, and viscoelastic dampers and bearing will jointly dissipate vibration energy; if the tension force exceeds the pressure of springs, the upper steel plate will detach from the core bearing, viscoelastic dampers will dissipate most of vibration energy, and the core bearing will be prevented from failure due to tension. Thus the shortcoming of the easiness of tension breakage for the ordinary rubber bearing is resolved in this device. In vertical direction, when pressing the device, the stiffness of the device is the pressure stiffness of the core bearing, it is really large enough just like the ordinary rubber bearing; when tensing the device, the stiffness of the device is sum of shear stiffness of the vertical viscoelastic dampers. Compared to the pressure stiffness, the tension stiffness is not large, but vertical viscoelastic dampers will really benefit to control the rocking effects due to dampers' symmetrical settings. For horizontal vibration, the device can isolate earthquake energy and prevent vibration energy from transferring to the upper structure like the ordinary rubber bearing. At the same time, viscoelastic dampers and the core viscoelastic bearing can dissipate the input earthquake energy due to the horizontal relative deformations of viscoelastic layers. It must be noted that the device can not only permit large deformation in horizontal direction but also permit large tension deformation in vertical direction. While large pressing deformation in vertical direction is not permitted due to vertical bearing capacity.

In the tested device, the core bearing consists of 35 viscoelastic layers with the thickness of 3 mm for each layer vulcanized alternatively with 34 layers of 2 mm steel plates. The diameter and the height of the core bearing are

Table 1  
The geometric parameters of the tested device

Parameters	Total height (mm)	Diameter (mm)	Number of VE layers	Thickness of VE layers (mm)	Number of steel plates	Thickness of steel plates (mm)
Bearing	173	70	35	3	34	2
Parameters	Outer cylinder (mm)	Inner cylinder (mm)	Height of VE layers	Thickness of VE layers (mm)	Number of dampers	Stiffness of springs (N/m)
Dampers	80	40	60	10	4	$1.3 \times 10^5$

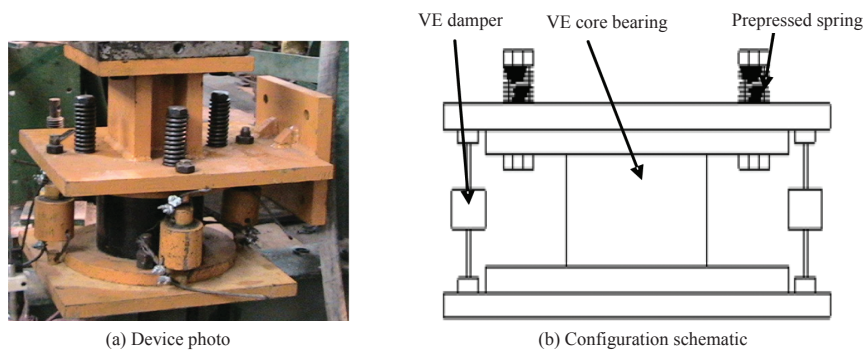


Fig. 1. Multi-dimensional earthquake isolation and mitigation device.

70 mm and 173 mm, respectively, as listed in Table 1. The cylinder viscoelastic dampers surrounded the core bearing is made up of two steel cylinders clamping the viscoelastic layer. The diameters of the inner and the outer cylinders are 40 mm and 80 mm, respectively. The thickness and height of the viscoelastic layer are 10 mm and 60 mm, respectively. Four pre-pressed springs with the stiffness of  $1.3 \times 10^5$  N/m enable providing 5500 N pressure. The viscoelastic material in the device is a high polymer, which has characteristics of both spring and fluid. The matrix of the polymer is brominated butyl rubber, and various kinds of additives including stearic acid, high abrasion furnace black, 200 mesh graphite powder, 2203 modified resin, etc. are added to improve the properties of viscoelastic materials. Under the harmonic displacement excitation, part of the damper's energy is stored as potential energy; the remaining part of the energy is dissipated as heat. Generally, the storage modulus  $G_1$  and the loss modulus  $G_2$  are used to describe the storage characteristic and the energy dissipation characteristic of viscoelastic devices, respectively [2]. In these tests, the viscoelastic material named ZN22, which is developed by Southeast University and Changzhou Earthquake Mitigation Company in China is adopted.

## 2.2. Test procedure

In order to measure vertical characteristic parameters including the initial stiffness, the energy dissipation stiffness, the energy dissipation per cycle and the equivalent damping ratio of the multi-dimensional earthquake isolation and mitigation device, numerous property tests on the device have been performed under different vertical excitations on a MTS closed-loop feedback hydraulic testing machine through displacement control mode in China, as shown in Fig. 2. In each test the device is subjected to twenty cycles of sinusoidal excitation with constant displacement amplitude and excitation frequency. Test duration of twenty cycles is chosen based on the idea that the duration of earthquakes is usually between several seconds to one minute. Outputs from the actuator load cell and displacement transducer are recorded by a high speed digital data acquisition system. Tests are conducted at displacements and frequencies selected to be appropriate for seismic applications. Four excitation frequencies, 0.1 Hz, 0.2 Hz, 0.5 Hz, and 1.0 Hz are applied to the device. For each excitation frequency, the excitation with the amplitudes of 1 mm, 2 mm, 4 mm, 6 mm, and 8 mm are performed, as shown in Table 2. The ambient temperature is set to room temperature 1 °C. In addition, the load and displacement data are used to plot the hysteresis loops in determining energy dissipation capability of the proposed multi-dimensional earthquake isolation and mitigation device. Only the loading under tension conditions for the device is applied, and this is due to the fact that the tension stiffness

Table 2  
The vertical loading program

No.	Frequency $f$ (Hz)	Displacement amplitude $d$ (mm)				
1	0.1	1	2	4	6	8
2	0.2	1	2	4	6	8
3	0.5	1	2	4	6	8
4	1.0	1	2	4	6	8



Fig. 2. Photograph of vertical loading test system.

and the compression stiffness of the device are different. Since the compression stiffness is far greater than the tension stiffness, the loading force will be excessive under the minor compressive displacement, which may easily lead to damage of the loading device. Displacement control method is adopted as the loading method under tension conditions for the device.

### 3. Test results and analysis

Vertical property tests data of the multi-dimensional earthquake isolation and mitigation device are plotted as force-displacement hysteresis loops point Representative curves for various test conditions are presented in Fig. 3. Figure 3(a) shows force-displacement hysteresis curves of the device under 0.1 Hz with five different amplitudes, and Fig. 3(b) shows those of the device under 6 mm amplitude with four different frequencies. Obviously frequency and amplitude have significant effects on vertical energy dissipation of the device. In order to reveal the effects of frequency or amplitude, a single steady-state cycle is selected from twenty cycles for each case. Hysteresis curves under amplitudes of 2 mm and 4 mm with different frequency excitations are plotted in Figs 4 and 5, respectively. The shapes of hysteresis curves under 1 mm, 6 mm and 8 mm amplitudes excitations are same as Figs 4 and 5. It can be seen that frequency has effect on center inclined line (i.e. the equivalent stiffness) and area of hysteresis curve (i.e. energy dissipation). Hysteresis curves under the frequencies, 0.2 Hz and 0.5 Hz, with different amplitude excitations are plotted in Figs 6 and 7, respectively. The shapes of hysteresis curves under 0.1 Hz and 1 Hz excitations are quite similar to the curves under 0.2 Hz and 0.5 Hz excitations shown as Figs 6 and 7. It can be seen that amplitude has also effect on center inclined line (i.e. the equivalent stiffness) and area of hysteresis curve (i.e. energy dissipation). The numerical comparison on these effects will be analyzed in the following.

It can be seen from these figures that the hysteresis loops consist of two parts: one is before the inflection points, which approximates an oblique line, and the slope of the oblique line reflects the stiffness of the pre-pressure of springs. The other is after the inflection point, which is formed due to the complex combination action of springs, small dampers and core bearing. Therefore, the vertical tension stiffness of the multi-dimensional earthquake isolation and mitigation device can be divided into the initial stiffness  $K_1$  and the energy dissipation stiffness  $K_2$ , which can be solved by the test hysteresis curves, as illustrated in Fig. 8. The initial stiffness  $K_1$ , the energy dissipation stiffness  $K_2$  and the vertical equivalent damping ratio  $\zeta$  can be obtained by

$$K_1 = \frac{F_A}{u_A} \quad (1)$$

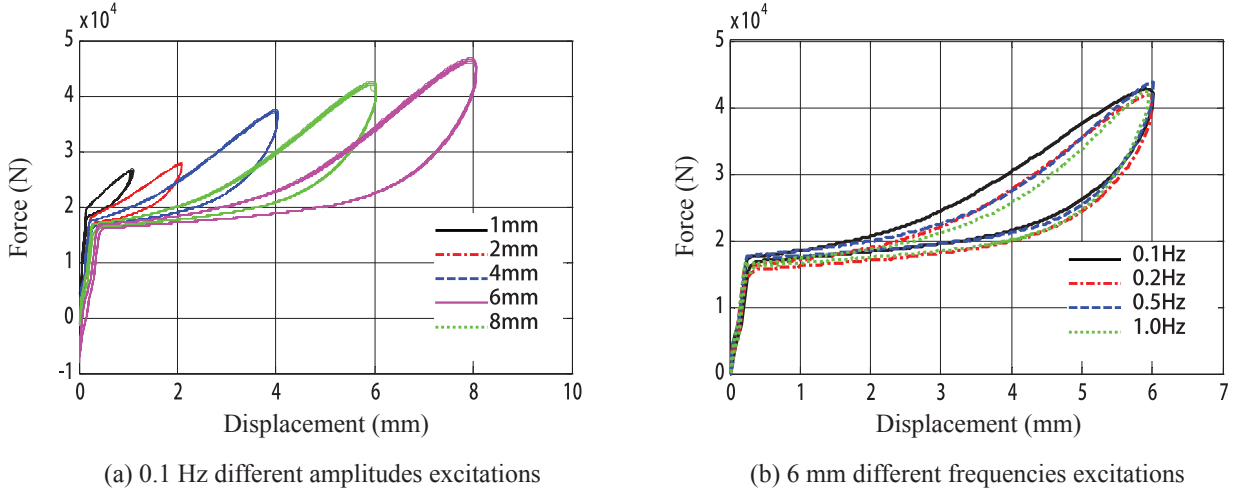


Fig. 3. Hysteresis curves under different excitation conditions.

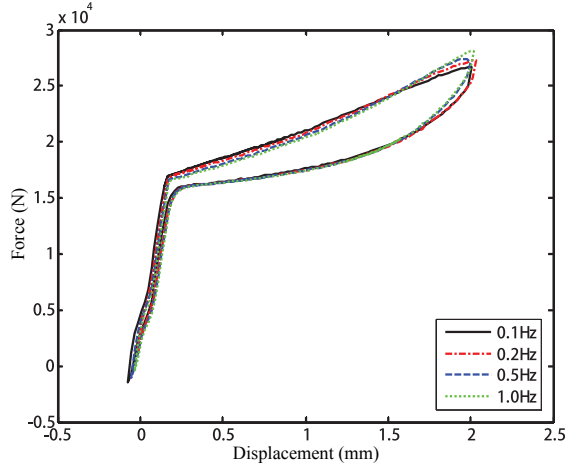


Fig. 4. Hysteresis curves under 2 mm amplitude with various frequency excitations.

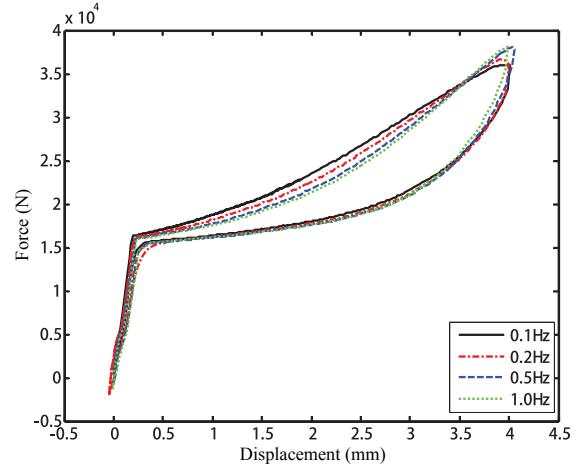


Fig. 5. Hysteresis curves under 4 mm amplitude with various frequency excitations.

$$K_2 = \frac{F_C - F_A}{u_C - u_A} \quad (2)$$

$$\zeta = \frac{E_d}{2\pi K_2 u_C^2} \quad (3)$$

where  $E_d$  is the vertical energy dissipation of the device, which can be determined by the test hysteresis loops using Matlab program,  $u_A, u_B, u_C, u_D, u_E$  and  $F_A, F_B, F_C, F_D, F_E$  are displacements and forces at A, B, C, D, E points in Fig. 8. Obviously, the vertical characteristic parameters can be denoted by the initial stiffness  $K_1$ , the energy dissipation stiffness  $K_2$  and the vertical equivalent damping ratio  $\zeta$ .

### 3.1. Excitation frequency effect

In order to show the effect of frequency on characteristic parameters, characteristic parameters including the initial stiffness  $K_1$ , the energy dissipation stiffness  $K_2$ , the energy dissipation per cycle  $E_d$  and the vertical equivalent

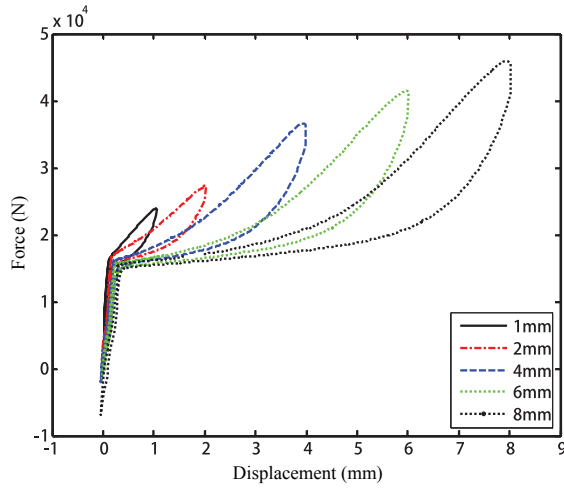


Fig. 6. Hysteresis curves under 0.2 Hz with various amplitudes excitations.

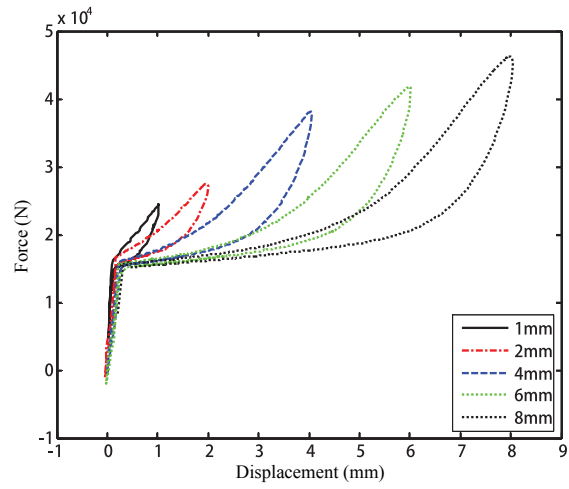


Fig. 7. Hysteresis curves under 0.5 Hz with various amplitude excitations.

damping ratio  $\zeta$  are calculated from the test hysteresis curves under different frequency excitations in accordance with Eqs (1)–(3). Figure 9 shows the characteristic parameters changing with frequency.

It can be seen from Fig. 9 that the initial stiffness  $K_1$  coming from the stiffness of viscoelastic bearing and four viscoelastic dampers increases slowly with increasing frequency. The energy dissipation stiffness  $K_2$  mainly governed by four viscoelastic dampers and springs has a trend similar to that of the initial stiffness  $K_1$ . Take 4 mm excitation displacement amplitude condition for example, when the frequency increases from 0.1 Hz to 0.2 Hz, 0.2 Hz to 0.5 Hz, 0.5 Hz to 1.0 Hz, and by every 0.1 Hz increasing frequency, the corresponding increases are 11.0%, 1.6%, 0.24% in the initial stiffness, and 7.7%, 0.98%, 0.4% in the energy dissipation stiffness, respectively. With increasing excitation frequency, the storage modulus and the loss modulus will increase [10], which will lead to increase of the initial stiffness and the energy dissipation stiffness. Energy dissipation per cycle  $E_d$  and the vertical equivalent damping ratio  $\zeta$  decrease slightly with increasing frequency, as also seen in Figs 4 and 5. Take 4 mm excitation displacement amplitude condition for example, when the frequency increases from 0.1 Hz to 0.2 Hz, 0.2 Hz to 0.5 Hz, 0.5 Hz to 1.0 Hz, and by every 0.1 Hz increasing frequency, the decreases are 3.1%, 3.0%, 2.1% in energy dissipation per cycle, and 10.1%, 3.9%, 2.5% in vertical equivalent damping ratio, respectively. This decrease mainly occurs in the upper part of the hysteresis loops, which may result from the flexibility of cables connecting between the upper steel plate and viscoelastic dampers, especially for hysteresis loops in high frequency vibration. Decrease of the damping ratio  $\zeta$  is primarily caused by two reasons, one is that energy dissipation per cycle  $E_d$  will decrease slightly in higher frequency, and the other is that the energy dissipation stiffness  $K_2$  in denominator part in Eq. (3) increase with increasing frequency.

### 3.2. Excitation amplitude effect

The test results of characteristic parameters of the multi-dimensional earthquake isolation and mitigation device with various amplitudes under different frequencies are show in Fig. 10. It can be seen from Fig. 10 that the initial stiffness  $K_1$  and the energy dissipation stiffness  $K_2$  decrease with increasing amplitude. Take 1.0 Hz excitation frequency condition for example, when the displacement amplitude increases from 1 mm to 2 mm, 2 mm to 4 mm, 4 mm to 6 mm, 6 mm to 8 mm, the corresponding initial stiffness  $K_1$  is decreased by 30.7%, 4.4%, 3.7%, 12.5%, and the energy dissipation stiffness  $K_2$  is decreased by 35.5%, 8.3%, 22.8%, 12.4%, respectively. This phenomenon may be caused by two reasons. One is due to that the energy dissipation per cycle  $E_d$  increase with increasing amplitude, these dissipation energy transfers into heat energy of viscoelastic material, which leads to temperature rise and this temperature rise will in turn cause decrease of shear stiffness of viscoelastic material. The other is that tests under different frequencies are firstly carried out, and then various excitation amplitude tests are carried out followed. As a result, the cables connecting the upper steel plate and viscoelastic dampers become flexible after long

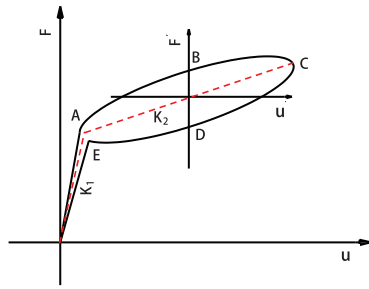


Fig. 8. Characteristics of the hysteresis curve of the device.

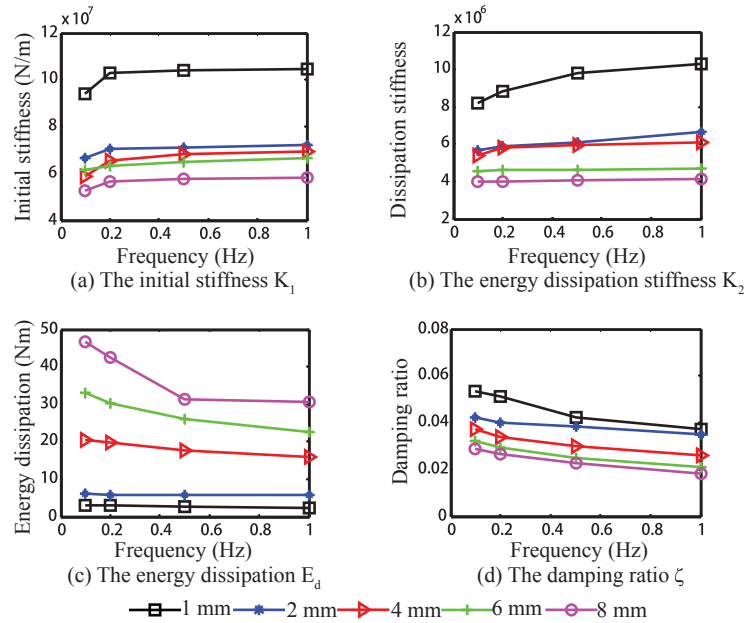


Fig. 9. Frequency's effect on characteristic parameters of the device.

period of tests. It can be imaged that the energy dissipation per cycle  $E_d$  increases with increasing amplitude, when the excitation amplitude increases, the hysteresis loops are becoming large. For instance, at the 1.0 Hz excitation frequency, with the displacement amplitude increasing from 1 mm to 2 mm, 2 mm to 4 mm, 4 mm to 6 mm, 6 mm to 8 mm, the corresponding energy dissipation per cycle  $E_d$  increase is 140.5%, 174.7%, 41.8%, 34.9%, respectively. On the contrary, the damping ratio  $\zeta$  decreases with increasing amplitude. For instance, at the 1.0 Hz excitation frequency, with the displacement amplitude increasing from 1 mm to 2 mm, 2 mm to 4 mm, 4 mm to 6 mm, 6 mm to 8 mm, the corresponding damping ratio  $\zeta$  decrease is 6.7%, 25.1%, 18.5%, 13.2%, respectively. This may be also caused by temperature rise of viscoelastic material under large amplitudes and decrease of tension forces in the cables connecting the upper steel plate and viscoelastic dampers. The transferred heat in vibration under large amplitudes is difficult to be radiated, which will lead to rise of temperature in viscoelastic material.

### 3.3. Theoretical simulation

The vertical characteristic parameters of the multi-dimensional earthquake isolation and mitigation device include the initial stiffness  $K_1$ , the energy dissipation stiffness  $K_2$ , energy dissipation per cycle  $E_d$  and the vertical equivalent damping ratio  $\zeta$ . It is desirable to deduce the corresponding formulas to simulate these parameters, especially for the initial stiffness  $K_1$ , the energy dissipation stiffness  $K_2$ , and the vertical equivalent damping ratio  $\zeta$ . It can be seen from Fig. 9 that amplitude effects on the initial stiffness, the energy dissipation stiffness, and the vertical equivalent damping ratio under different frequencies can be simply described by polynomial functions. And frequency effects on the initial stiffness, the energy dissipation stiffness, and the vertical equivalent damping ratio under different amplitudes can be represented by exponent functions. Therefore the initial stiffness  $K_1$ , the energy dissipation stiffness  $K_2$ , and the vertical equivalent damping ratio  $\zeta$  can be expressed as follows.

$$K_1 = \varphi_{K_1}(f) \cdot \psi_{K_1}(u) \quad (4)$$

$$K_2 = \varphi_{K_2}(f) \cdot \psi_{K_2}(u) \quad (5)$$

$$\zeta = \varphi_{\zeta}(f) \cdot \psi_{\zeta}(u) \quad (6)$$

where  $\varphi(f)$  is the polynomial function related to frequency,  $\psi(u)$  is the exponent function relative to displacement amplitude,  $f$  is the frequency and  $u$  is the displacement amplitude. In accordance with test results of 1 mm, 4 mm,

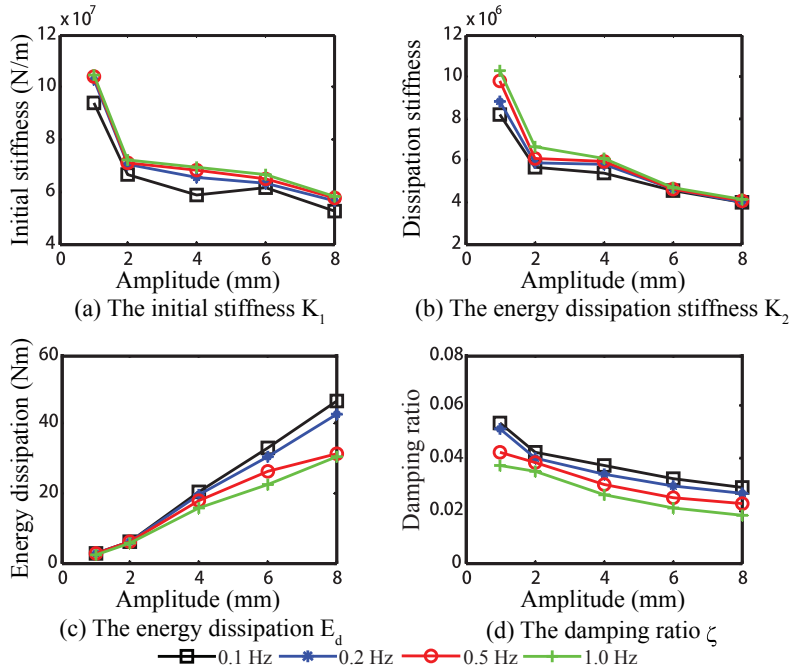


Fig. 10. Amplitude's effect on characteristic parameters of the device.

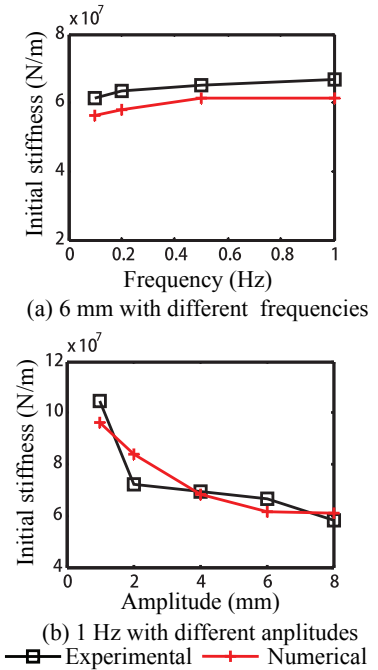


Fig. 11. Comparison of initial stiffness between experimental and numerical results.

8 mm displacement amplitudes with different frequencies and 0.2 Hz, 0.5 Hz excitation frequencies with different amplitudes, the following formulas can be obtained.

$$K_1 = \left[ (-0.2278f^2 + 0.3487f + 0.9207) \cdot e^{0.0122u^2 - 0.1751u + 2.3852} \right] \times 10^7 \text{ N/m} \quad (7)$$

$$K_2 = \left[ (-0.1336f^2 + 0.2686f + 0.9265) \cdot e^{0.0109u^2 - 0.2002u + 2.3226} \right] \times 10^6 \text{ N/m} \quad (8)$$

$$\zeta = \left[ (0.3281f^2 - 0.7383f + 1.2256) \cdot e^{0.0081u^2 - 0.1628u + 1.6694} \right] \times 10^{-2} \quad (9)$$

In order to verify the effectiveness of the above formulas, the numerical results of the initial stiffness  $K_1$ , the energy dissipation stiffness  $K_2$ , and the vertical equivalent damping ratio  $\zeta$  under 6 mm displacement amplitude with different frequencies are obtained by Eqs (7)–(9). Comparisons between numerical and experimental results are plotted in Figs 11–13. Figure 11 shows the comparison between numerical and experimental results for the initial stiffnesses  $K_1$ . The maximum error occurs in 0.1 Hz under 6 mm amplitude excitation, the experimental and numerical initial stiffnesses are  $6.148 \times 10^7 \text{ N/m}$  and  $5.622 \times 10^7 \text{ N/m}$ , respectively, and the error is 8.5%. The maximum error occurs in 2 mm amplitude under 1 Hz excitation, the experimental and numerical initial stiffnesses are  $7.237 \times 10^7 \text{ N/m}$  and  $8.369 \times 10^7 \text{ N/m}$  with the error 15.6%. Figure 12 shows the numerical and experimental results comparison for the energy dissipation stiffness  $K_2$ . The maximum error occurs in 0.1 Hz under 6 mm amplitude excitation, the experimental and numerical energy dissipation stiffnesses are  $4.553 \times 10^6 \text{ N/m}$  and  $4.319 \times 10^6 \text{ N/m}$ , respectively, giving the error is 5.1%. The maximum error occurs in 1 mm amplitude under 1 Hz excitation, the experimental and numerical energy dissipation stiffnesses are  $10.115 \times 10^6 \text{ N/m}$  and  $8.668 \times 10^6 \text{ N/m}$  with the error 14.3%. Figure 13 shows the numerical and experimental results comparison for the vertical equivalent damping ratio  $\zeta$ . The maximum error occurs in 0.1 Hz under 6 mm amplitude excitation, the experimental and numerical equivalent damping ratios are 3.21% and 3.09%. The maximum error occurs in 2 mm amplitude under 1 Hz excitation, the experimental and numerical energy dissipation stiffnesses are 3.47% and 3.23%. It can be seen that the proposed formulas can describe the initial stiffness  $K_1$ , the energy dissipation stiffness  $K_2$ , and the vertical equivalent damping ratio changing with excitation amplitude and frequency.

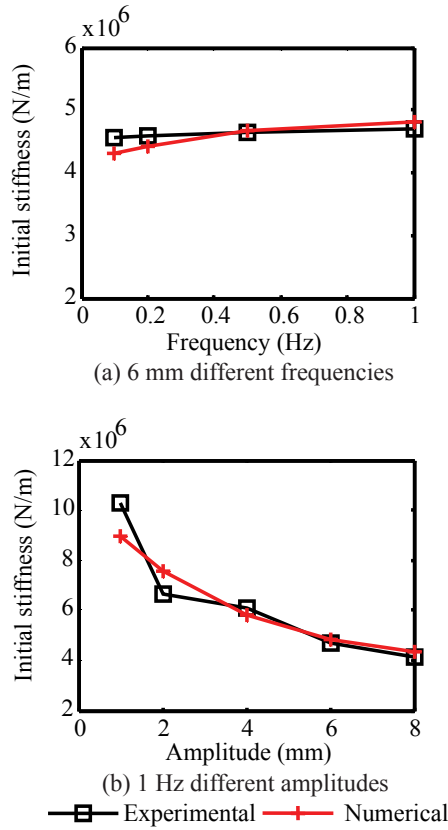


Fig. 12. Comparison of energy dissipation stiffness between experimental and numerical results.

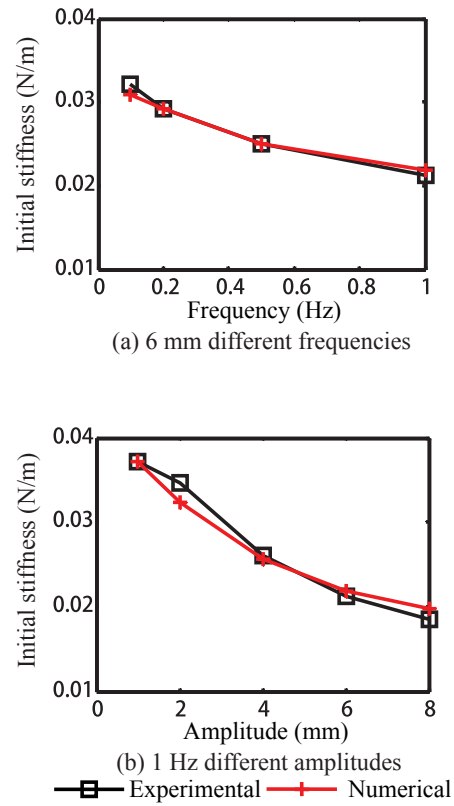


Fig. 13. Comparison of damping ratio between experimental and numerical results.

For the new kind of multi-dimensional earthquake isolation and mitigation device, its properties including the initial stiffness  $K_1$ , the energy dissipation stiffness  $K_2$ , the energy dissipation per cycle  $E_d$  and the vertical equivalent damping ratio  $\zeta$  are affected by excitation frequency, excitation amplitude and environmental temperature. These effects mainly come from the effects of these factors on viscoelastic material in the device. Temperature effect on viscoelastic material is introduced in study on horizontal properties of the device (Part I). The stiffness will decrease with increasing temperature, and the energy dissipation per cycle  $E_d$  and the vertical equivalent damping ratio  $\zeta$  will have the optimum values under some a temperature. Here the effects of excitation frequency and excitation amplitude are mainly studied. It can be concluded that as the excitation frequency increases, both the initial stiffness  $K_1$  and the energy dissipation stiffness  $K_2$  increase slightly, while the energy dissipation per cycle  $E_d$  and the vertical equivalent damping ratio  $\zeta$  decrease slightly; and as the excitation amplitude increases, the initial stiffness  $K_1$ , the energy dissipation stiffness  $K_2$  and the vertical equivalent damping ratio  $\zeta$  decrease.

#### 4. Conclusions

In this study, a new kind of multi-dimensional earthquake isolation and mitigation device is designed and tested, the characteristic parameters of the multi-dimensional earthquake isolation and mitigation device are obtained and some formulas are proposed to simulate their properties. Several conclusions can be made through experimental and numerical studies.

- (1) The multi-dimensional earthquake isolation and mitigation device has a remarkable capability for vertical energy dissipation. The test hysteresis loop consists of two parts. One is prior to the inflection points, which the oblique line is produced by the pre-pressure of the springs; the other is similar to an ellipse after the inflection

point, which is formed due to the complex combination action of springs, small dampers and core bearing. The properties of the multi-dimensional earthquake isolation and mitigation device can be characterized by the initial stiffness  $K_1$ , the energy dissipation stiffness  $K_2$ , the energy dissipation per cycle  $E_d$  and the vertical equivalent damping ratio  $\zeta$ .

- (2) As the excitation frequency increases, both the initial stiffness  $K_1$  and the energy dissipation stiffness  $K_2$  increase slightly, while the energy dissipation per cycle  $E_d$  and the vertical equivalent damping ratio  $\zeta$  decrease slightly.
- (3) As the excitation amplitude increases, the initial stiffness  $K_1$ , the energy dissipation stiffness  $K_2$  and the vertical equivalent damping ratio  $\zeta$  decrease.
- (4) The proposed formulas are capable of simulating the initial stiffness  $K_1$ , the energy dissipation stiffness  $K_2$ , and the vertical equivalent damping ratio of the multi-dimensional earthquake isolation and mitigation device.

## Acknowledgment

Financial supports for this research are provided by National Natural Science Foundation of China with granted number 90915004, Jiangsu Province Natural Science Foundation with granted number BK2011063, Doctoral Fund of Ministry of Education of China with granted number 20090092110012 and Jiangsu Province 333 Talents Program. These supports are gratefully acknowledged.

## References

- [1] A. Kashiwazaki and T. Fujiwaka, Feasibility tests on a three-dimensional base isolation system incorporating hydraulic mechanism, *American Society of Mechanical Engineers, PVP* **445(2)** (2002), 11–18.
- [2] J.K. Kim, J.G. Ryu and L. Chung, Seismic performance of structures connected by viscoelastic dampers, *Engineering Structures* **28(2)** (2006), 183–195.
- [3] Ministry of Construction of P.R. China, Code for seismic design of buildings: GB 50011-2001, China Construction Industry Press, 2001.
- [4] W.L. Qu and Q. Zhou, Tensional-vertical seismic response control of multi-story structure with intelligent compound base-isolation system, *Earthquake Engineering and Engineering Vibration* **23(5)** (2003), 187–189.
- [5] T. Shimada and J. Suhara, Three dimensional seismic isolation system for next-generation nuclear power plant with rolling seal type air spring and hydraulic rocking suppression system, in: *Proceedings of the ASME Pressure Vessels and Piping Conference*, Denver, Colorado, USA, 8, 2005, 183–190.
- [6] T. Somaki, A. Miyamoto et al., Development of 3-dimensional base isolation system with coned disk spring, *Seismic Engineering* **428(2)** (2001), 49–55.
- [7] J.M. Suhara, Y.M. Okada et al., Development of three dimensional seismic isolation devices with laminated rubber bearing and rolling seal type air spring, *American Society of Mechanical Engineers, PVP* **445(2)** (2002), 43–48.
- [8] S.S. Xiong and J.F. Chen, Nonlinear analysis of multi-dimensional seismic response in 3D base isolated structure, *Journal of Huazhong University of Science and Technology* **32(12)** (2004), 81–84.
- [9] Z.D. Xu, X. Zeng, X.H. Huang and L.H. Lu, Experimental and numerical studies on a new multi-dimensional earthquake isolation and mitigation device: horizontal properties, *Science China Series E-Tech Science* **53 (10)** (2010), 2658–2667.
- [10] G.Q. Zhou and X.M. Liu, *Viscoelastic Theory*, Press of University of Science and Technology of China, Hefei, China, 1996.

